



Correlation of minimum apparent diffusion coefficient with maximum standardized uptake on fluorodeoxyglucose PET-CT in patients with rectal adenocarcinoma

Hale Çolakoğlu Er, Ayşe Erden, N. Özlem Küçük, Ethem Geçim

PURPOSE

The aim of this study was to retrospectively assess the correlation between minimum apparent diffusion coefficient (ADC_{min}) values obtained from diffusion-weighted magnetic resonance imaging (MRI) and maximum standardized uptake values (SUV_{max}) obtained from positron emission tomography-computed tomography (PET-CT) in rectal cancer.

MATERIALS AND METHODS

Forty-one patients with pathologically confirmed rectal adenocarcinoma were included in this study. For preoperative staging, PET-CT and pelvic MRI with diffusion-weighted imaging were performed within one week (mean time interval, 3 ± 1 day). For ADC measurements, the region of interest (ROI) was manually drawn along the border of each hyperintense tumor on $b=1000$ s/mm² images. After repeating this procedure on each consecutive tumor-containing slice to cover the entire tumoral area, ROIs were copied to ADC maps. ADC_{min} was determined as the lowest ADC value among all ROIs in each tumor. For SUV_{max} measurements, whole-body images were assessed visually on transaxial, sagittal, and coronal images. ROIs were determined from the lesions observed on each slice, and SUV_{max} values were calculated automatically. The mean values of ADC_{min} and SUV_{max} were compared using Spearman's test.

RESULTS

The mean ADC_{min} was $0.62\pm 0.19\times 10^{-3}$ mm²/s (range, 0.368– 1.227×10^{-3} mm²/s), the mean SUV_{max} was 20.07 ± 9.3 (range, 4.3–49.5). A significant negative correlation was found between ADC_{min} and SUV_{max} ($r=-0.347$; $P=0.026$).

CONCLUSION

There was a significant negative correlation between the ADC_{min} and SUV_{max} values in rectal adenocarcinomas.

Diffusion-weighted imaging (DWI) is a widely used technique for disease evaluation in oncology (1, 2). In rectal cancer, the applications of DWI include tumor detection, tumor characterization, distinguishing tumor tissue from nontumor tissue, and monitoring and predicting treatment response (3–8). For local staging of rectal cancer, adding DWI to conventional magnetic resonance imaging (MRI) yields better identification of tumor borders and locoregional lymph nodes than conventional MRI alone (9, 10).

The apparent diffusion coefficient (ADC) map obtained from DWI shows the freedom of water diffusion, and values calculated on the map are useful parameters in tissue characterization. By performing diffusion-weighted (DW) MRI with at least two diffusion weightings, or b values, the differential signal attenuation at different b values can be used to calculate the ADC (2). Regardless of the tumor type and location, the ADC values reflect tumor morphology, including the cellular density, integrity of cell membrane, and nuclear-to-cytoplasm ratio (11, 12).

Positron emission tomography/computed tomography (PET-CT) has become a crucial method in cancer imaging, both for diagnosis and staging, as well as for offering prognostic information based on tumor response. In PET-CT, the standardized uptake value (SUV) is a measure of fluorodeoxyglucose (FDG) uptake, which has been shown to be helpful in establishing the metabolic activity level of a tumor (13–15).

Both ADC and SUV have been used as important imaging parameters to supplement visual interpretation. To our knowledge, few studies have evaluated the relationship between ADC and SUV in cancer patients (16–18). The aim of the present study was to retrospectively assess the correlation between the minimum ADC (ADC_{min}) on DWI and maximum SUV (SUV_{max}) values from FDG PET-CT in rectal cancer.

Materials and methods

Patients

Between March 2010 and November 2012, 53 consecutive patients underwent pelvic MRI using a 3.0 Tesla system for baseline local staging of rectal tumors. Inclusion criteria for the present study consisted of histopathologically (biopsy) proven rectal adenocarcinoma and the presence of correlative PET-CT. Exclusion criteria were histologic subtypes other than adenocarcinoma (including mucinous adenocarcinoma) according to the current World Health Organization classification of colorectal cancer (19) and insufficient magnetic resonance (MR) image quality (e.g., owing to metal implants or movement artifacts). Twelve patients were excluded for the following reasons: severe motion artifacts on DW images (n=1), histopathologic diagnosis of mucinous adenocarcinoma (n=2),

From the Departments of Radiology (H.Ç.E., A.E. ✉ ayse.erden@medicine.ankara.edu.tr), Nuclear Medicine (N.Ö.K.), and General Surgery (E.G.), Ankara University School of Medicine, Ankara, Turkey.

Received 12 June 2013; revision requested 9 July 2013; revision received 15 July 2013; accepted 19 July 2013.

Published online 8 October 2013.
DOI 10.5152/dir.2013.13275

Table. Pulse sequence parameters

Parameter	Sagittal T2-weighted TSE	Axial T2-weighted TSE	Oblique axial T2-weighted TSE (High resolution)	Oblique coronal T2-weighted TSE (High resolution)	T1-weighted fat suppressed contrast-enhanced
Matrix size	384×307	320×240	320×240	320×240	320×240
Slice thickness (mm)	3.5	5.0	3.5	3.5	3.5
Distance factor	15%	20%	14%	14%	14%
Repetition time (ms)	4500	5450	5460	5180	495
Echo time (ms)	104	93	85	85	12
Echo trains per slice	13	8	12	15	39
Flip angle (°)	120	150	149	130	140
Reduction factor	2	2	2	2	2
Averages	2	3	3	3	2
FoV (mm)	220×220	220×220	200×200	200×200	200×200
Orientation	Sagittal	Axial	Oblique axial	Oblique coronal	Oblique axial
Bandwidth (Hz/Px)	250	260	260	260	260
Acquisition time (min and s)	4 min, 5 s	2 min, 18 s	3 min, 24 s	4 min	3 min, 17 s

FoV, field of view; TSE, turbo spin echo.

and absence of correlative PET-CT (n=9). Forty-one consecutive patients (24 males, 17 females; age range, 41–79 years [mean age, 59 years]) who met the inclusion criteria were enrolled in the current study. All patients provided written informed consent. Our Institutional Ethics Committee approved this retrospective study.

MR techniques

All patients were fasted from food for periods of 5–6 hours before examination to prevent stimulation of bowel peristalsis. No intravenous antiperistaltic agent was administered. Rectal cleansing was not performed. Air insufflation or a water enema was not carried out for rectal distension.

The patients underwent MRI using 3.0 Tesla whole-body system (MAGNETOM Verio, Siemens, Erlangen, Germany) and a phased-array body coil. The imager operates with a maximum gradient strength of 45 mT/m and a slew rate of 200 mT/m/s in all three directions. Conventional MR images and DW images were acquired during the same procedure. The MR imaging examination consisted of standard sagittal and axial T2-weighted turbo spin-echo images, high-resolution oblique axial and oblique coronal T2-weighted images, axial DW

images, and contrast-enhanced fat suppressed T1-weighted axial images. All pulse sequence parameters other than those of DWI used in this study are listed in detail in Table. DW images with three different b values (50, 400, and 1000 s/mm²) were obtained in the axial plane using a single-shot multi-slice echoplanar imaging (EPI) sequence with spectral adiabatic inversion recovery fat suppression and the following parameters: repetition time/echo time, 6800/75 ms; EPI factor, 78; field of view, 360×271 mm; matrix size, 130×104; slice thickness, 5 mm; distance factor, 20%; averages, 4; reduction factor, 2; and receiver bandwidth, 2402 Hz/Px. The acquisition time for the DWI was 4 min and 25 s.

The PET-CT scanner used in this study was a Discovery ST PET/CT scanner (General Electric, Milwaukee, Wisconsin, USA). The CT device had eight rows of detectors. The CT data were used for attenuation correction. To maintain a normal “fasting glucose level”, the patients were instructed not to eat food for six hours before the PET-CT imaging. Patients with diabetes mellitus were required to fast for four hours before the examination and allowed to continue to take their antidiabetic medication or to administer insulin. In patients whose preparation was adequate, the blood glucose level was checked at the imag-

ing center to ensure that the patients' glucose level was not too low or high. If the level was still greater than 150 mg/dL, crystallized insulin was administered to the patient intramuscularly to lower the blood glucose level under 150 mg/dL. Next, 1000 cc of low-density oral contrast agent were administered to the patients to aid in the evaluation of gastrointestinal FDG uptake and facilitate confident exclusion or diagnosis of luminal and mural disease. In all patients, 0.15 mCi/kg of the intravenous tracer (radiopharmaceutical) fluorine-18 FDG (¹⁸F-FDG) was administered. After the injection of ¹⁸F-FDG, the patients were requested to rest in a semirecumbent arm chair as calmly as they can for 50–60 min. At the end of the resting period, the patients were asked to empty their bladder because intense bladder activity can impair the interpretation of lesions in the pelvis. All the patients were scanned from the vertex to the midfemur. After routine imaging, additional views of the suspicious uptake area were obtained whenever necessary. All participants underwent pelvic DWI and FDG PET-CT within one week (mean time interval, 3±1 days).

Image interpretation

The ADC maps were automatically generated using a monoexponential de-

cay model, including all three b-values at Siemens Software Version syngo MR B17. Regions of interest (ROIs) covering the tumor were drawn manually on DW images with $b=1000$ s/mm². On each slice, the high signal intensity of tumor boundaries was traced, and ROIs were copied to the corresponding ADC map to measure ADC values. ADC_{min} was the lowest value of the ADC obtained from the tumor-containing slices.

For SUV_{max} measurements, whole-body images from FDG PET-CT in axial, sagittal, and coronal planes were evaluated visually. The ROI for the SUV measurements was drawn manually around each tumor on all consecutive slices that contained the lesion, and SUV_{max} values were calculated automatically.

Statistical analysis

Because the data shown were not in a normal distribution, Spearman's correlation (nonparametric test) was employed to analyze the relationship between the ADC_{min} and SUV_{max} values. Statistical analysis was performed using a commercially available software (Statistical Package for Social Sciences, version 15.0, SPSS Inc., Chicago, Illinois, USA). *P* values less than

0.05 were deemed to indicate a statistically significant difference.

Results

Tumor thickness ranged between 1.3 and 2.5 cm (mean size, 1.7 cm). The mean ADC_{min} of tumors was $0.62 \pm 0.19 \times 10^{-3}$ mm²/s (range, 0.368–1.227 $\times 10^{-3}$ mm²/s). The mean SUV_{max} of tumors was 20.07 ± 9.3 (range, 4.3–49.5). There was a negative correlation between ADC_{min} and SUV_{max} ($r = -0.347$, $P = 0.026$). The graph shows the negative correlation between values of ADC_{min} and SUV_{max} (Fig. 1). An example of our cases is presented in Fig. 2.

Discussion

Advancing technology allows the acquisition of physiological and metabolic information that complements the anatomic information provided by conventional imaging methods. Quantification of the level of signal attenuation and uptake values is used mainly for making comparisons between tissues. In the present study, DWI of rectal cancer allows quantitative evaluation of the ADC. We found a negative correlation between ADC_{min} and SUV_{max} values. In our study, we includ-

ed only the minimum ADC value measurements. The present definition of minimum ADC is the lowest value selected from multiple ROIs drawn manually along the border of the lesion on each consecutive tumor-containing slices, including the whole tumor volume, not the lowest value corresponding to a pixel in one ROI surrounding the mass. The regions with minimum ADCs have been suggested to reflect the highest tumor cell density or the most proliferative portion of the tumor (20).

Malignant lesions are characterized by high signal intensity on DW images with high b value and exhibit lower ADC values. Diffusion of water within malignant tissue from the extracellular to the intracellular compartment is relatively restricted. Several investigators have found an inverse correlation between the ADC and tumor cellularity (21). Recently, it has been reported that lower ADC values were associated with a more aggressive tumor profile in rectal cancer (22). Although MRI provides high-resolution anatomic information, PET adds information concerning the metabolic activity of lesions. Tumoral uptake is estimated by SUV, reflecting metabolically active tissue volume. Glucose is a critical nutrient for proliferating cells. Thus, it may not be surprising that tumor cells, to meet the increased requirements of proliferation, often display fundamental changes in pathways of energy metabolism and glucose uptake (23).

Studies of the correlation between ADC_{min} and SUV_{max} are few. Cafagna et al. (16) measured SUV and ADC values of lesions to determine the possible correlation between PET-CT and DWI in 38 patients with malignancy. However, they did not find a significant correlation between these two parameters. This result may be the consequence of including different types of malignant processes in the study or may be due to the method used to calculate ADC values. Ho et al. (17) found no significant correlation between ADC_{min} and SUV_{max} in patients with primary cervical tumor. In that study, however, a significantly inverse correlation between the relative ADC_{min} (defined as ADC_{min}/ADC mean ratio) and relative SUV_{max} was observed in patients with adeno-

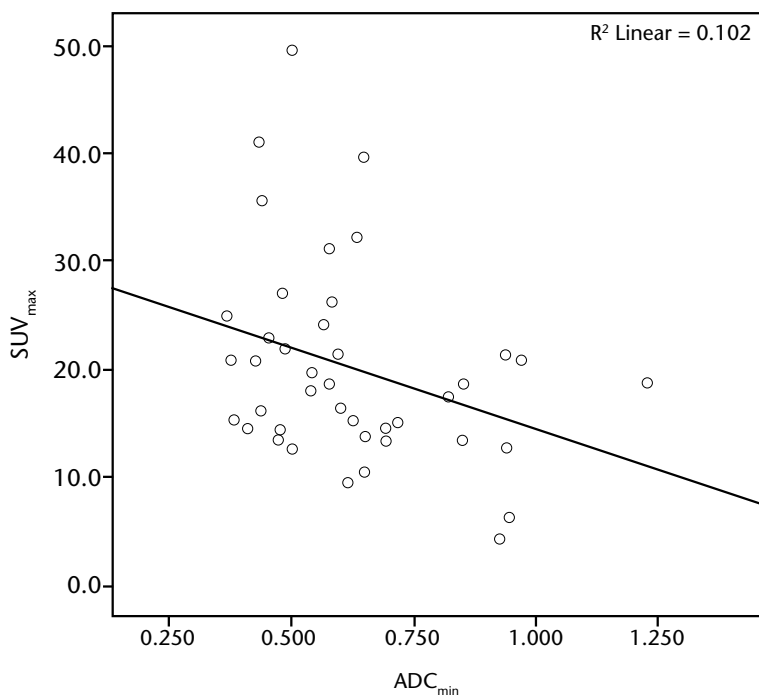


Figure 1. Negative correlation between ADC_{min} and SUV_{max}. The ADC is expressed in units of 10^{-3} mm²/s.

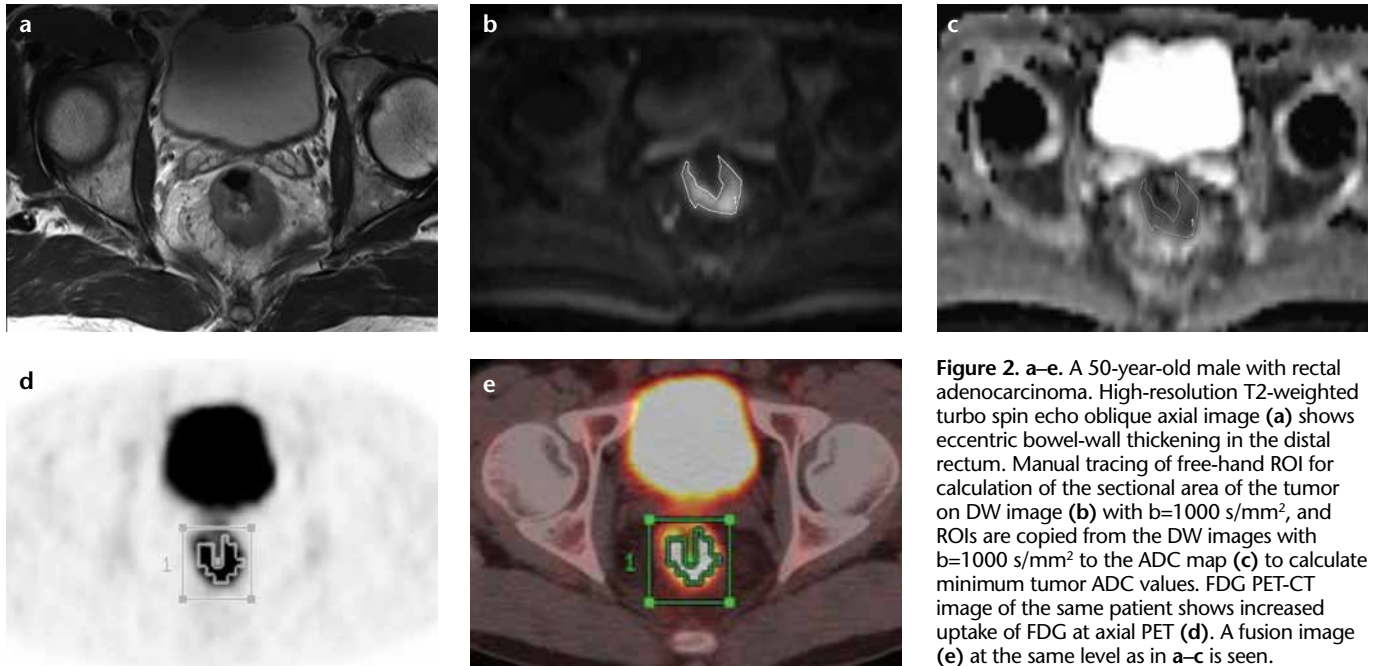


Figure 2. a–e. A 50-year-old male with rectal adenocarcinoma. High-resolution T2-weighted turbo spin echo oblique axial image (a) shows eccentric bowel-wall thickening in the distal rectum. Manual tracing of free-hand ROI for calculation of the sectional area of the tumor on DW image (b) with $b=1000$ s/mm², and ROIs are copied from the DW images with $b=1000$ s/mm² to the ADC map (c) to calculate minimum tumor ADC values. FDG PET-CT image of the same patient shows increased uptake of FDG at axial PET (d). A fusion image (e) at the same level as in a–c is seen.

carcinoma/adenosquamous carcinoma ($r=-0.685$; $P = 0.0012$). The authors suggest that DWI and FDG PET-CT might play a complementary role for the clinical assessment of this cancer type (17). Gu et al. (18) assessed correlations between parameters on DWI and FDG PET-CT in rectal cancer. Significant negative correlations were found between ADC_{min} and SUV_{max} ($r=-0.450$, $P = 0.009$), and between ADC mean and SUV mean ($r=-0.402$, $P = 0.020$). A significant positive correlation was found between the total diffusivity index (TDI) obtained from DWI and total lesion glycolysis (TLG) obtained from FDG PET-CT ($r=0.634$; $P < 0.001$). The authors concluded that the significant negative correlation between ADC and SUV suggests an association between tumor cellularity and metabolic activity in primary rectal adenocarcinoma (18).

Neoadjuvant chemoradiotherapy has become a standard treatment for locally advanced rectal cancer. However, this application is not beneficial for all patients. The patients who do not respond to preoperative chemoradiotherapy are exposed to unnecessary toxicities of the neoadjuvant therapy, and resection of their primary tumor is delayed (24). Ippolito et al. (25) evaluated the correlation between the changes in SUV_{max} and ADC before and

after neoadjuvant therapy in patients with locally advanced rectal cancer. The best predicted cutoff values for response are an SUV_{max} of 4.4 and an ADC of 1.28×10^{-3} mm²/s with sensitivity, specificity, accuracy, negative predictive value, and positive predictive values of 77.3%, 88.9%, 80.7%, 61.5%, and 94.4%, respectively. They concluded that the absolute values of SUV_{max} and ADC of rectal lesions after chemoradiotherapy were the best parameters to define the response to treatment (25).

Our study had some limitations. We assessed only minimum ADC values and maximum SUV in our study. Combining multiple parameters such as the mean ADC, tumor volume, total diffusivity index, mean SUV, and total lesion glycolysis as imaging biomarkers might provide more comprehensive information regarding the tumoral process.

Several factors affect the values measured as ADC and SUV (26, 27). ADC measurements are subject to institutional differences and intraobserver variability. The ROI is an important consideration because small variations in ROI size or placement may result in non-negligible variations in ADC that may substantially influence the results. Size and location influence tumor ADC measurements in rectal cancer (28). It has been shown that ADC

measurements of the “whole tumor volume” provide the most reproducible and dependable results for clinical applications (28). In our study, we used this method for consecutive tumor-containing slices. The histologic subtype of rectal carcinoma may also affect ADC values. Mucinous tumors are known to have a low cellular density and high extracellular mucin component. It has been established that mucinous adenocarcinoma of the rectum shows higher ADC values than well-differentiated adenocarcinoma due to its low cellularity (29). There are also diverse factors influencing SUV determination, such as ROI shape, partial-volume effects, reconstruction method and parameters for the scanner type, tissue state factors (type and extent of disease, vascularity, organ usage, urine management policy), time of SUV evaluation, body size, and competing transport effects (serum glucose and protein levels) (27). Understanding these factors and knowledge of potential interpretive pitfalls will help to avoid mistakes.

In conclusion, ADC_{min} and SUV_{max} are inversely correlated parameters in patients with rectal cancer. They reflect the most cellular and metabolically active portions of the tumoral lesions and provide physiopathological information as quantifiable data.

Conflict of interest disclosure

The authors declared no conflicts of interest.

References

1. Türkbey B, Aras Ö, Karabulut N, et al. Diffusion-weighted MRI for detecting and monitoring cancer: a review of current applications in body imaging. *Diagn Interv Radiol* 2012; 18:46–59.
2. Koh DM, Collins DJ, Orton MR. Intravoxel incoherent motion in body diffusion-weighted MRI: reality and challenges. *AJR Am J Roentgenol* 2011; 196:1351–1361. [\[CrossRef\]](#)
3. Ichikawa T, Erturk SM, Motosugi U, et al. High-b-value diffusion-weighted MRI in colorectal cancer. *AJR Am J Roentgenol* 2006; 187:181–184. [\[CrossRef\]](#)
4. Shinya S, Sasaki T, Nakagawa Y, Guiqing Z, Yamamoto F, Yamashita Y. The efficacy of diffusion-weighted imaging for the detection of colorectal cancer. *Hepatogastroenterology* 2009; 56:128–132.
5. Kilickesmez O, Atilla S, Soyulu A, et al. Diffusion-weighted imaging of the rectosigmoid colon: preliminary findings. *J Comput Assist Tomogr* 2009; 33:863–866. [\[CrossRef\]](#)
6. Song I, Kim SH, Lee SJ, Choi JY, Kim MJ, Rhim H. Value of diffusion-weighted imaging in the detection of viable tumour after neoadjuvant chemoradiation therapy in patients with locally advanced rectal cancer: comparison with T2 weighted and PET/CT imaging. *Br J Radiol* 2012; 85:577–586. [\[CrossRef\]](#)
7. Kim SH, Lee JM, Hong SH, et al. Locally advanced rectal cancer: added value of diffusion-weighted MR imaging in the evaluation of tumor response to neoadjuvant chemo- and radiation therapy. *Radiology* 2009; 253:116–125. [\[CrossRef\]](#)
8. Lambregts DM, Vandecaveye V, Barbaro B, et al. Diffusion-weighted MRI for selection of complete responders after chemoradiation for locally advanced rectal cancer: a multicenter study. *Ann Surg Oncol* 2011; 18:2224–2231. [\[CrossRef\]](#)
9. Mizukami Y, Ueda S, Mizumoto A, et al. Diffusion-weighted magnetic resonance imaging for detecting lymph node metastasis of rectal cancer. *World J Surg* 2011; 35:895–899. [\[CrossRef\]](#)
10. Lambregts DM, Maas M, Riedl RG, et al. Value of ADC measurements for nodal staging after chemoradiation in locally advanced rectal cancer—a per lesion validation study. *Eur Radiol* 2011; 21:265–273. [\[CrossRef\]](#)
11. Castillo M, Smith JK, Kwock L, Wilber K. Apparent diffusion coefficients in the evaluation of high-grade cerebral gliomas. *AJNR Am J Neuroradiol* 2001; 22:60–64.
12. Nonomura Y, Yasumoto M, Yoshimura R, et al. Relationship between bone marrow cellularity and apparent diffusion coefficient. *J Magn Reson Imaging* 2001; 13:757–760. [\[CrossRef\]](#)
13. Palma P, Conde-Muñoz R, Rodríguez-Fernández A, et al. The value of metabolic imaging to predict tumour response after chemoradiation in locally advanced rectal cancer. *Radiat Oncol* 2010; 5:119. [\[CrossRef\]](#)
14. Grassetto G, Marzola MC, Minicozzi A, Al-Nahhas A, Rubello D. F-18 FDG PET/CT in rectal carcinoma: where are we now? *Clin Nucl Med* 2011; 36:884–888. [\[CrossRef\]](#)
15. Grassetto G, Capirci C, Marzola MC, et al. Colorectal cancer: prognostic role of 18F-FDG-PET/CT. *Abdom Imaging* 2012; 37:575–579. [\[CrossRef\]](#)
16. Cafagna D, Rubini G, Iuele F, et al. Whole-body MR-DWIBS vs. [18F]-FDG-PET/CT in the study of malignant tumors: a retrospective study. *Radiol Med* 2012; 117:293–311. [\[CrossRef\]](#)
17. Ho KC, Lin G, Wang JJ, Lai CH, Chang CJ, Yen TC. Correlation of apparent diffusion coefficients measured by 3T diffusion-weighted MRI and SUV from FDG PET/CT in primary cervical cancer. *Eur J Nucl Med Mol Imaging* 2009; 36:200–208. [\[CrossRef\]](#)
18. Gu J, Khong PL, Wang S, Chan Q, Law W, Zhang J. Quantitative assessment of diffusion-weighted MR imaging in patients with primary rectal cancer: correlation with FDG-PET/CT. *Mol Imaging Biol* 2011; 13:1020–1028. [\[CrossRef\]](#)
19. Lanza G, Messerini L, Gafà R, Risio M; Gruppo Italiano Patologi Apparato Digerente (GIPAD); Società Italiana di Anatomia Patologica e Citopatologia Diagnostica/International Academy of Pathology, Italian division (SIAPEC/IAP). Colorectal tumors: the histology report. *Dig Liver Dis* 2011; 43:S344–355. [\[CrossRef\]](#)
20. Lee EJ, terBrugge K, Mikulis D, et al. Diagnostic value of peritumoral minimum apparent diffusion coefficient for differentiation of glioblastoma multiforme from solitary metastatic lesions. *AJR Am J Roentgenol* 2011; 196:71–76. [\[CrossRef\]](#)
21. Higano S, Yun X, Kumabe T, et al. Malignant astrocytic tumors: clinical importance of apparent diffusion coefficient in prediction of grade and prognosis. *Radiology* 2006; 241:839–846. [\[CrossRef\]](#)
22. Curvo-Semedo L, Lambregts DM, Maas M, Beets GL, Caseiro-Alves F, Beets-Tan RG. Diffusion-weighted MRI in rectal cancer: apparent diffusion coefficient as a potential noninvasive marker of tumor aggressiveness. *J Magn Reson Imaging* 2012; 35:1365–1371. [\[CrossRef\]](#)
23. Garber K. Energy deregulation: licensing tumors to grow. *Science* 2006; 312:1158–1159. [\[CrossRef\]](#)
24. Garajová I, Di Girolamo S, de Rosa F, et al. Neoadjuvant treatment in rectal cancer: actual status. *Chemother Res Pract* 2011; 2011:839742.
25. Ippolito D, Monguzzi L, Guerra L, et al. Response to neoadjuvant therapy in locally advanced rectal cancer: assessment with diffusion-weighted MR imaging and 18FDG PET/CT. *Abdom Imaging* 2012; 37:1032–1040. [\[CrossRef\]](#)
26. Feuerlein S, Pauls S, Juchems MS, et al. Pitfalls in abdominal diffusion-weighted imaging: how predictive is restricted water diffusion for malignancy. *AJR Am Roentgenol* 2009; 193:1070–1076. [\[CrossRef\]](#)
27. Thie JA. Understanding the standardized uptake value, its methods, and implications for usage. *J Nucl Med* 2004; 45:1431–1434.
28. Lambregts DM, Beets GL, Maas M, et al. Tumour ADC measurements in rectal cancer: effect of ROI methods on ADC values and interobserver variability. *Eur Radiol* 2011; 21:2567–2574. [\[CrossRef\]](#)
29. Nasu K, Kuroki Y, Minami M. Diffusion-weighted imaging findings of mucinous carcinoma arising in the ano-rectal region: comparison of apparent diffusion coefficient with that of tubular adenocarcinoma. *Jpn J Radiol* 2012; 30:120–127. [\[CrossRef\]](#)